

Large epitaxial bi-axial strain induces a Mott-like phase transition in VO₂

Salinporn Kittiwatanakul, Stuart A. Wolf, Jiwei Lu*

Salinporn Kittiwatanakul

Department of Physics, University of Virginia, Charlottesville, VA, U.S., 22904

Prof. S. A. Wolf

Department of Physics and Department of Materials Science and Engineering, University of Virginia, Charlottesville, VA, U.S., 22904

Prof. Jiwei Lu

Department of Materials Science and Engineering, University of Virginia, Charlottesville, VA, U.S., 22904

E-mail: jl5tk@virginia.edu

Keywords: vanadium dioxide, metal insulator transition, strongly correlation, Mott transition

The metal insulator transition (MIT) in VO₂ has been an important topic for recent years. It has been generally agreed that the mechanism of the MIT in bulk VO₂ is considered to be a collaborative Mott-Peierls transition, however the effect of the strain on the phase transition is much more complicated. In this study the effect of the large strain on the properties of VO₂ films was investigated. One remarkable result is that highly strained epitaxial VO₂ thin films were rutile in the insulating state as well as in the metallic state. These highly strained VO₂ films underwent an electronic phase transition without the concomitant Peierls transition. Our results also show that a very large tensile strain along the *c*-axis of rutile VO₂ resulted in a phase transition temperature of ~ 433 K, much higher than in any previous report. Our findings elicit that the metal insulator transition in VO₂ can be driven by an electronic transition alone, rather the typical coupled electronic-structural transition.

1. Introduction

The metal-insulator transition (MIT) is an intriguing property of vanadium dioxide (VO₂), which can be of benefit in many electronic and optical applications of sensing and switching. Bulk VO₂ undergoes a first order phase transition from a monoclinic structure (*MI*) to a rutile structure (*R*) at ~ 340 K, which is accompanied by drastic changes in the electric and optical conductivities. The very abrupt changes in physical properties lead to many potential ultrafast optical and electrical switching applications. It has been generally agreed that the mechanism

of the MIT in bulk VO₂ is considered to be a collaborative Mott-Peierls transition, however the effect of strain on the phase transition is much more complicated. Various types of strains such as macro-strains (mechanical strains, epitaxial strains etc.) and micro-strains via chemical substitutions in the lattice have been exploited to modify the phase transition. Recently reports revealed that single crystal VO₂ nanobeams under uniaxial strain exhibited a complex blend of insulating phases including the *M1*, *M2* and triclinic (*T*) phases near the MIT.^[1,2] Similarly, the micro-strain in the lattice induced by the chemical doping of Al, also resulted in the meta-stable *M2* phase in free-standing VO₂ films near room temperature.^[3] In contrast, epitaxial strain in thin film VO₂ from the crystal clamping with the substrate revealed a quite different picture of the phase transition. Despite the large lattice mismatch (~3.7 %) along the *c*-axis between the rutile TiO₂ and the VO₂ film, as summarized in table I, the experimental results by Muraoka *et al.*^[4] showed a strong correlation between the transition temperature (T_{MIT}) and the uniaxial strain along the *c*-axis of VO₂ (R), and the correlation was opposite to that predicted by the Peierls (structural) mechanism.^[5] Laverock *et al.*^[6] have observed a Mott-like transition with a large tensile strain along the c_R axis in VO₂ using soft x-ray spectroscopy, that demonstrated the absence of the large structural distortion near the phase transition, previously observed in bulk and moderately strained VO₂. Epitaxial films under bi-axial strain also demonstrated a very pronounced anisotropy in optical and transport properties,^[7,8] as a result of the formation of unidirectional stripe states in which the semiconducting and metallic states coexisted.^[9]

In this study, we grew epitaxial VO₂ films with thickness from 5~ 17 nm on various single crystal substrates to obtain very high epitaxial strains. As a result, the maximum T_{MIT} reached in this study is > 430 K, which is higher than previous reports, with 4 orders of magnitude change in the resistivity. Intriguingly, Raman spectroscopy revealed that the structures of VO₂ films grown on TiO₂ in the insulating states resembled metallic rutile VO₂, instead of the *M1*

phase observed when the films were grown on *c*-plane sapphire.

2. Results and Discussion

2.1 Microstructure characterization

In this study, epitaxial VO₂ films with thickness from 5~ 17 nm were grown on various single crystal substrates. The AFM images are shown in **Figure 1a**. The root-mean-square roughnesses of the films are also summarized in **Table 1**. AFM has revealed the smooth and uniform surface, and there are no cracks or pinholes. There are some signs of island growth mode of VO₂ for the very thin samples deposited 10 minutes or less, which is due to the large lattice mismatch between the film and the substrate. The grain size also increases with the film thickness.

The out-of-plane (2θ) XRD scans showed that the (020) peaks of monoclinic VO₂ were coupled to the (0006) peaks of the Al₂O₃ substrate as seen in figure 1b, and the VO₂ films deposited were highly textured and VO₂ was the only phase detected in wide-range 2θ scans, there are no other oxides grown on the substrate. As the films get thicker, the (020) VO₂ peaks shift to higher 2θ values, which mean the lattice parameter *b* (for monoclinic phase) gets smaller for thicker film (*b* is reported in table 1). The Al₂O₃ substrate has hexagonal symmetry, and the structure of VO₂ deposited on top is monoclinic, which can have three preferred in-plane orientations according to the substrate and film crystal structures. The in-plane lattice spacing of bulk VO₂ is larger than that of Al₂O₃, hence an in-plane compressive strain is introduced for the film deposited on the Al₂O₃ substrate.

Regarding to the VO₂ grown on TiO₂ substrates, the full epitaxial relationship of the films to the substrates was obtained due to the common rutile structure for both VO₂ and TiO₂. The lattice parameters of bulk VO₂ are smaller than that of the TiO₂ substrate, hence this introduces an in-plane tensile strain due to this lattice mismatch.^[10] Figure 1b also shows the out-of-plane XRD scans of the VO₂/(100) TiO₂ samples. The (200) peak in the VO₂ diffraction is coupled to the (200) peak of the TiO₂ substrate, and it is the only peak detected in the wide-range

E_{11} (E_{100}) is ~ 200 GPa,^[11] and E_{12} (E_{110}) ~ 90 GPa.^[12] However, there was a report on various simulated parameters, E_{ij} , for single crystal VO₂.^[13] The epitaxial strains were calculated from

$\frac{\Delta L_i}{L_i}$, i.e. $\varepsilon_1 = \frac{a - a_{bulk}}{a_{bulk}}$, where a is the measured lattice parameter along a -axis of VO₂ (R).

For further analysis, Eqn. 1 can be reduced to:

$$\begin{aligned}\sigma_1 &= E_{11}\varepsilon_1 + E_{12}\varepsilon_2 + E_{13}\varepsilon_3 \\ \sigma_2 &= E_{12}\varepsilon_1 + E_{11}\varepsilon_2 + E_{13}\varepsilon_3 \\ \sigma_3 &= E_{13}\varepsilon_1 + E_{13}\varepsilon_2 + E_{33}\varepsilon_3\end{aligned}\quad (2)$$

From Hooke's law, the bi-axially strained thin film boundary condition is applied according to the substrate orientation. It is stress-free along the out-of-plane direction, i.e. perpendicular to the film surface. For VO₂/(100) TiO₂, the condition $\sigma_1 = 0$, yields

$$\varepsilon_3 = \frac{E_{11}(-\varepsilon_1) + E_{12}(-\varepsilon_2)}{E_{13}}. \text{ We determined } \varepsilon_i \text{ from the measured lattice parameters,}^{[10]}$$

which agrees well with this formula. Both ε_1 and ε_2 are negative (compressive strains), while ε_3 is positive (tensile strain). As the in-plane tensile strain ε_3 decreased, the out-of-plane compressive strain ε_1 became more negative; hence the in-plane compressive strain ε_2 became less negative, approaching zero.

For VO₂/(001) TiO₂, the conditions $\sigma_1 = \sigma_2$, and $\sigma_3 = 0$, give $\varepsilon_1 = \varepsilon_2$, and $\varepsilon_3 = -\frac{2E_{13}}{E_{33}}\varepsilon_1$, respectively. The measured lattice parameters also agree with these conditions.^[10] As the out-plane lattice parameter c_R decreased, the in-plane lattice parameter a_R increased. However, the measured out-of-plane strain ε_3 fluctuates around zero with a declining tendency, when it should be negative (compressive), as the in-plane strains ε_1 and ε_2 are both positive (tensile). The result could also mean that $E_{33} \gg E_{13}$.

For VO₂/(011) TiO₂, the condition $\sigma_{[011]} = 0$, results in $\sigma_2 = -\sigma_3$, hence

$$\varepsilon_3 = \frac{(E_{11} + E_{13})(-\varepsilon_2) - (E_{12} + E_{13})\varepsilon_1}{(E_{13} + E_{33})}. \text{ In principle, from the substrate clamping effect, } \varepsilon_1 \text{ is}$$

positive (tensile). The measured lattice parameters showed that ε_2 is negative (compressive), and ε_3 is positive (tensile).^[10] As ε_3 was relaxed, ε_2 became more compressive, then the tensile strain ε_1 should increase faster than the compressive strain ε_2 (assuming $E_{11} > E_{12}$). The trend demonstrated by the evolution in the lattice parameters as a function of the film thickness agree with these nominal conditions but the rate of change does not agree very well, which implies that E_{12} may be larger than E_{11} .

In comparison, the stress and strain in the uniaxially strained nanobeams is very simple.^[1,2] The uniaxial stress has the following stress tensor form:

$$\sigma = \begin{pmatrix} 0 & 0 & 0 \\ 0 & 0 & 0 \\ 0 & 0 & P \end{pmatrix} \quad (3)$$

Where P is the mechanical stress applied along c -axis of monoclinic VO_2 . When P is tensile (positive), the strain along c is tensile, and the strains along $[100]$ and $[010]$ are compressive. When P is compressive (negative), the strains along $[100]$, $[010]$, and $[001]$ change their signs accordingly.

2.3. Raman spectra

Figure 2 shows Raman spectra of VO_2/TiO_2 compared to that of $\text{VO}_2/c\text{-Al}_2\text{O}_3$. The spectra of VO_2/TiO_2 shown here (before substrate/background subtraction) were dominated by the TiO_2 signal at room temperature and at 150 °C. The room temperature spectra of VO_2/TiO_2 did not reveal any insulating MI features, but rather showed small diffusive peaks after background subtraction, similar to what has been reported for metallic VO_2 (*Rutile phase*) and to what we observed in the high temperature spectra of $\text{VO}_2/c\text{-Al}_2\text{O}_3$. Even though the lattice parameter c (i.e. c -strain) varies for the different film thicknesses, the Raman spectroscopy shows the MI phase only for all $c\text{-Al}_2\text{O}_3$ samples at lower temperature, and the ω_0 peak shifts slightly from 615 to 617 cm^{-1} as the strain along $[001]$ $MI\text{-VO}_2$ was increasing. The tendency of the peak shift agrees with a previous report on VO_2 micro-beams,^[1] but the T phase and $M2$ phase were not observed in any of our samples.

For the VO₂/TiO₂ samples, only the insulating-*R* phase was observed and there wasn't any frequency shift at room temperature. The crystal structure of the substrate, i.e. the symmetry and the lattice parameters, plays an important role in determining the symmetry of epitaxial films and the strains along different in-plane directions, hence for the TiO₂ substrates, only the *R*-phase VO₂ was observed in the given thickness range. As a comparison, the free-standing nanobeams can adopt a crystal structure either with a different symmetry (*M2*, *T*) to accommodate the applied mechanical strain.^[2]

2.4. Metal insulator transition

Figure 3 summarizes the transport behavior of VO₂ deposited on TiO₂ and sapphire substrates. The transport behaviors of ~13 nm VO₂ deposited on various substrates are shown in figure 3a. The inset shows an image of the device with Ti/Au top contacts for the measurements. The film deposited on (100) TiO₂ has the highest T_{MIT} ~358 K, while the film on (0001) Al₂O₃ has a T_{MIT} ~332 K, the film on (011) TiO₂ has a T_{MIT} ~321 K and the film on (001) TiO₂ has the lowest T_{MIT} ~ 305 K. A similar shift was explained using the strain from the TiO₂ substrate in a previous report.^[4] In this current experiment, a systematic study of the thickness dependence of T_{MIT} on various substrates is reported to further understand how to control the strain via different film thicknesses. The resistivities as a function of temperature for various thicknesses of VO₂ grown on (100) TiO₂ are shown in figure 3b. As the films get thinner (more strained), the T_{MIT} shifts to higher temperature. The 4.9 nm film has an unusually high T_{MIT} (~ 433 K) as seen in figure 3b inset. The T_{MIT} were determined from resistivity as a function of temperature measurements on all other films.^[10]

A phase diagram is proposed in **Figure 4** for the bi-axially strained VO₂. It shows the regimes of the metallic phase, the semiconductor phase, and the region of coexistence of the rutile phase, that is based on hysteresis loop and anisotropy of the transport data collected from previous reports.^[7-9,14] In this phase diagram, the T_{MIT} shows a rather linear relationship

with the c -axis strain, which is in good agreement with a previous report.^[4] It is worthy noting that that the lattice parameter c in Muraoka's report was calculated assuming the volume of the unit cell was conserved. In this study, the lattice parameters were directly determined from XRD 2θ scans. This new phase diagram extracted from the experimental data confirms the prediction, using cluster-dynamic mean field theory that investigates the effect of the epitaxial strain on the electronic structure of rutile VO₂,^[5] where the strain dependence of $d_{||}$ state has also been confirmed by Laverock *et al.*^[15] Not only does it show that the rutile phase can stabilize both metallic and insulating states, but also predicts that the coexistence of both insulating and metallic phases, for large values of the on-site Coulomb interaction potential (U). Experimentally, the photoemission spectroscopy on bi-axially strained VO₂ on TiO₂ substrates showed a weak insulating gap as well as the suppression of orbital redistribution across the transition, which lead to a conclusion of a more Mott-like MIT with the absence of a structural distortion, i.e. Peierls transition.^[6] In highly strained epitaxial films (with the thickness much larger than what were reported here), an intriguing unidirectional strip state was observed with mixed metallic and insulating phases via scattering-type scanning near-field optical microscopy,^[9] which serve as strong evidence for the coexistence of rutile insulating and metallic phases.

The films on (100) TiO₂ substrates have the largest strain, resulting the highest T_{MIT} , while the films on (001) TiO₂ substrates have the smallest strain, and the lowest T_{MIT} . Being the most strained films, the VO₂/(100) TiO₂ samples experience the largest shift in the transition temperature (T_{MIT}) as the thickness varies, on the other hand, the thickness has the smallest effect on the c -strain and the T_{MIT} for the (011) and (001) samples. This is because the c -mismatch is much larger than the a -mismatch, hence the (100) samples get the largest (in-plane) strain from the substrate clamping effect, and can relax much faster than (011) and (001) samples. The T_{MIT} can be modified in a wide range from 300 - 440 K, via strain

manipulation by both substrate choice and thickness, which enhances the useful temperature range of the MIT for potential applications.

3. Conclusion

In summary, the properties of single-phase strained VO₂ thin films were studied on various single crystal substrates. Raman spectra showed that epitaxial VO₂ films grown on TiO₂ single crystal substrates were the rutile phase in both insulating state and metallic state, despite various orientations, instead of the *MI* state observed on *c*-plane sapphire. The strained VO₂ underwent an electronic phase transition without the Peierls transition as observed in single crystal and polycrystalline VO₂. A new phase diagram of bi-axially strained VO₂ was proposed, in which only the rutile VO₂ is presented. Secondly, a large increase in T_{MIT} up to 433 K was observed for VO₂/(100) TiO₂, much higher than any previous report, while the T_{MIT} of VO₂/(001) TiO₂ was reduced to 305 K, with the large, 3-4 orders of magnitude change in resistivity preserved. The ability to tune the T_{MIT} using strain engineering that has been demonstrated in this work extends the potential temperature range for the use of VO₂ in nanoelectric devices.

4. Experimental Section

Reactive Target Ion Beam Deposition (RBTIBD) was used to grow VO₂ thin film on (100), (001), (011) TiO₂ and *c*-Al₂O₃ substrates. The systematic study of growth conditions can be found elsewhere.^[16] The Raman spectroscopy with a 488 nm laser source, was conducted at room temperature and at 150 °C. To characterize the transport behavior of the films, photolithography was used to fabricate 250 × 250 μm² top contacts with a separation of 5 μm. The Ohmic contact was 100 nm Au / 10 nm Ti, deposited by electron beam evaporation. The temperature dependence of the *dc* resistivity was measured with a heating/cooling rate of 2 K/min, from 250 to 400 K.

Acknowledgements

We thank Y. Wang and L.-k. Tsui for help with the Raman spectroscopy, and J. Florro for the discussions. We acknowledge the support by the Nanoelectronics Research Initiative (NRI) and VMEC.

- [1] J. M. Atkin, S. Berweger, E. K. Chavez, M. B. Raschke, J. Cao, W. Fan, and J. Wu, *Phys. Rev. B*, **2012**, 85, 020101.
- [2] J. H. Park, J. M. Coy, T. S. Kasirga, C. Huang, Z. Fei, S. Hunter, and D. H. Cobden, *Nature*, **2013**, 500, 431.
- [3] E. Strelcov, A. Tselev, I. Ivanov, J. D. Budai, J. Zhang, J. Z. Tischler, I. Kravchenko, S. V. Kalinin, and A. Kolmakov, *Nano Lett.*, **2012**, 12, 6198.
- [4] Y. Muraoka and Z. Hiroi, *Appl. Phys. Lett.*, **2002**, 80, 583 (2002).
- [5] B. Lazarovits, K. Kim, K. Haule, and G. Kotliar, *Phys. Rev. B*, **2010**, 81, 115117.
- [6] J. Laverock, A. R. H. Preston, D. Newby, K. E. Smith, S. Sallis, L. F. J. Piper, S. Kittiwatanakul, J. W. Lu, S. A. Wolf, M. Leandersson, and T. Balasubramanian, *Phys. Rev. B*, **2012**, 86, 195124.
- [7] E. Abreu, M. Liu, J. Lu, K. G. West, S. Kittiwatanakul, W. Yin, S. A. Wolf, and R. D. Averitt, *New J. Phys.*, **2012**, 14, 083026.
- [8] S. Kittiwatanakul, J. Lu, and S. A. Wolf, *Appl. Phys. Express*, **2011**, 4, 091104.
- [9] M. K. Liu, M. Wagner, E. Abreu, S. Kittiwatanakul, A. McLeod, Z. Fei, M. Goldflam, S. Dai, M. M. Fogler, J. Lu, S. A. Wolf, R. D. Averitt, and D. N. Basov, *Phys. Rev. Lett.*, **2013**, 111, 096602.
- [10] See Supplementary Document.
- [11] H. Baumgart, *Private communication*.
- [12] N. Sepúlveda, A. Rúa, R. Cabrera, and F. Fernández, *Appl. Phys. Lett.*, **2008**, 92, 191913.
- [13] W. Fan, J. Cao, J. Seidel, Y. Gu, J. W. Yim, C. Barrett, K. M. Yu, J. Ji, R. Ramesh, L. Q. Chen, and J. Wu, *Phys. Rev. B*, **2011**, 83, 235102.
- [14] J. Lu, K. G. West, and S. A. Wolf, *Appl. Phys. Lett.*, **2008**, 93, 262107.
- [15] J. Laverock, L. F. J. Piper, A. R. H. Preston, B. Chen, J. McNulty, K. E. Smith, S. Kittiwatanakul, J. W. Lu, S. A. Wolf, P. A. Glans, and J. H. Guo, *Phys. Rev. B*, **2012**, 85, 081104.
- [16] K. G. West, J. Lu, J. Yu, D. Kirkwood, W. Chen, Y. Pei, J. Claassen, and S. A. Wolf, *J. Vac. Sci. Technol. A*, **2008**, 26, 133.

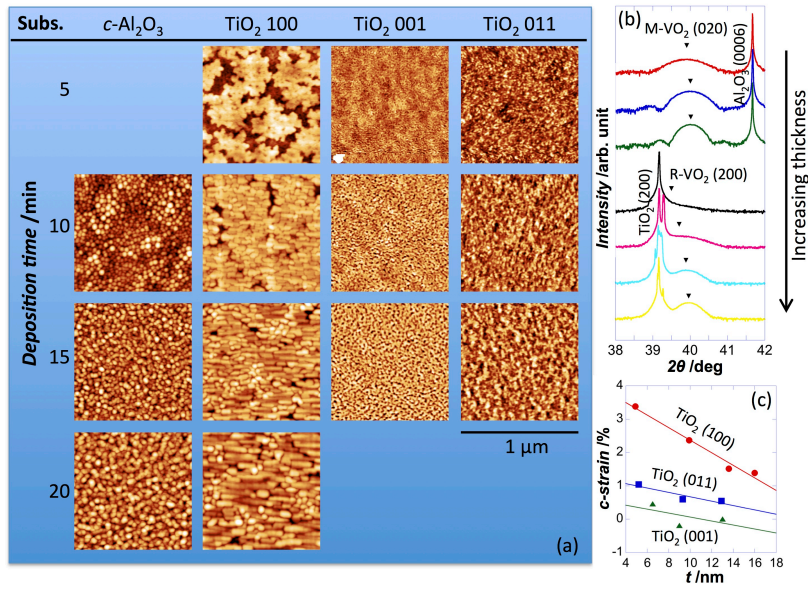


Figure 1. (a) $1 \times 1 \mu\text{m}^2$ AFM images of all samples (normalized scale for better detail). (b) 2θ XRD scans of $\text{VO}_2/c\text{-Al}_2\text{O}_3$ and $\text{VO}_2/(100) \text{TiO}_2$, showing VO_2 peak couple to the substrate peak, and peak shifts as film thickness increases. (c) c_R strain vs. film thickness (t) for $\text{VO}_2/(100) \text{TiO}_2$ samples.

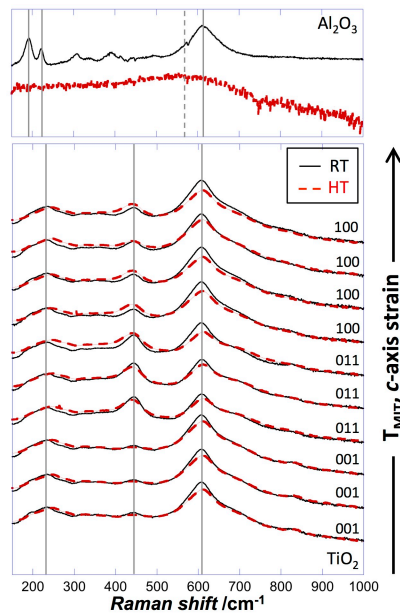


Figure 2. Top: Raman spectra of VO_2 thin film grown on $c\text{-Al}_2\text{O}_3$ (for reference) showing insulating MI structure at room temperature and showing metallic rutile structure at 150°C respectively. Bottom: Raman spectra of VO_2 thin film grown on TiO_2 , measured at room temperature and 150°C .

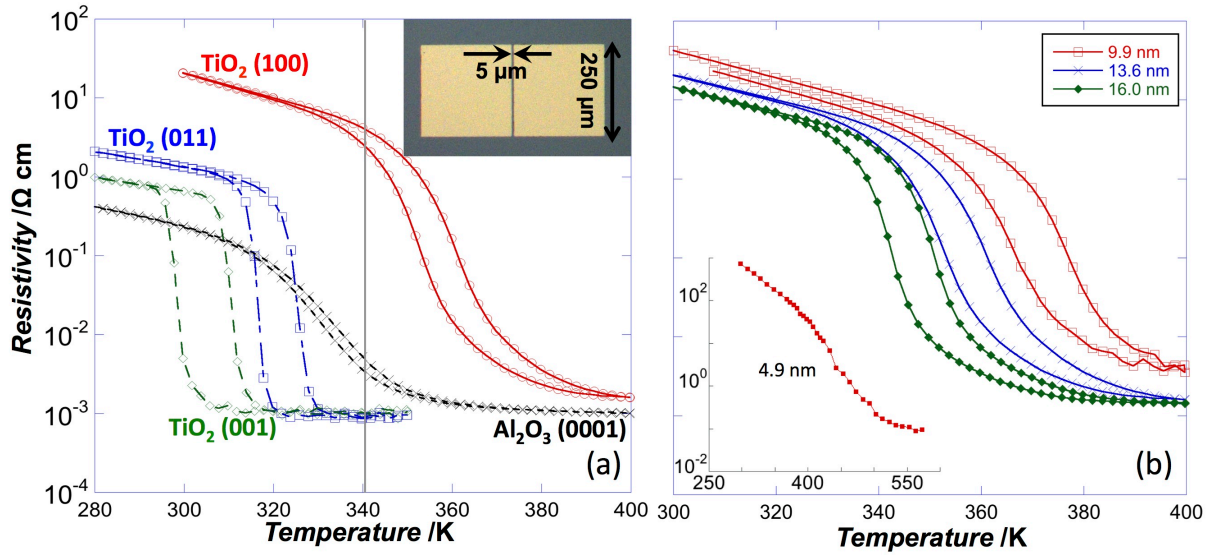


Figure 3. (a) Resistivity as a function of temperature of 15-min deposited (12.7-13.6 nm) VO₂ on various substrates, the vertical solid line indicate T_{MIT} of bulk, the inset shows device image with Ti/Au top contacts and 5 μ m \times 250 μ m VO₂ channel. (b) Resistivity as a function of temperature of various thicknesses VO₂/(100) TiO₂, the inset shows the extended temperature measurement of the thinnest film.

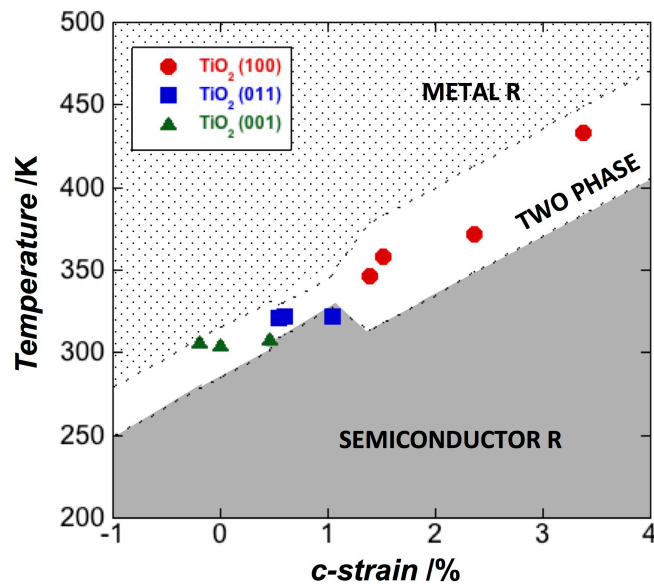


Figure 4. Phase diagram of rutile VO₂ collected from T_{MIT} as a function of uniaxial c -strain, hysteresis loop, and transport anisotropy of VO₂ deposited on various TiO₂ substrates.

Table 1. Summary of thickness, RMS roughness, and lattice parameter (b or c)

Deposit time (min)	c-Al ₂ O ₃			TiO ₂ (100)			TiO ₂ (011)			TiO ₂ (001)		
	t (nm)	RMS (nm)	b (Å)	t (nm)	RMS (nm)	c (Å)	t (nm)	RMS (nm)	c (Å)	t (nm)	RMS (nm)	c (Å)
5				4.9	0.81	2.9493	5.2	0.19	2.8826	6.5	0.12	2.8660
10	8.7	1.60	4.5132	9.9	0.88	2.9204	9.3	0.24	2.8699	9.0	0.25	2.8475
15	12.7	0.40	4.5028	13.6	1.10	2.8961	12.9	0.34	2.8684	13.0	0.49	2.8529
20	17.0	0.60	4.5014	16.0	1.45	2.8924						

Supporting Information

Large epitaxial bi-axial strain induces a Mott-like phase transition in VO₂

*Salinporn Kittiwantanakul, Stuart A. Wolf, Jiwei Lu**

The lattice parameters of bulk VO₂ are smaller than that of the TiO₂ substrate, hence this introduces an in-plane tensile strain due to this lattice mismatch as summarized in **Table S1**. Based on the lattice mismatch, we have calculated the critical thickness (H_c) for VO₂ grown on various orientations of rutile TiO₂. Below the critical thickness, the epitaxial film is fully strained thanks to the mismatch. Once the thickness exceeds the critical thickness, the misfit dislocations form spontaneously to relax the epitaxial strain, hence the strain of film shows a strong dependence to the film thickness.

Table S1. Lattice parameters, in-plane spacing, and critical thickness of VO₂, TiO₂ (Å)

Material	a	c	d_{011}	d_{110}
R-VO ₂	4.5546	2.8528	2.4177	3.2206
TiO ₂	4.5936	2.9582	2.4871	3.2482
Mismatch (%)	0.86	3.69	2.87	0.86
H_c	2.6595	0.3861	0.4211	1.8806

The out-of-plane, in-plane 2θ scans and in-plane Phi (ϕ) scans were performed to provide the lattice parameters, and confirm epitaxial growth on TiO₂ substrates. **Figure S1a** shows the ϕ scan showing VO₂ and TiO₂ peaks for the (101) plane, which confirms the epitaxial growth of VO₂ thin films with rutile crystal structure. The lattice parameters, a , b , and c were directly extracted from the three 2θ scans for each of the samples grown on TiO₂ as shown in figure S1b-d. The lattice parameter c approaches the bulk value, as the film gets thicker for all films

grown on TiO₂ substrates; while the (100) samples have the largest uniaxial strain along $\langle 001 \rangle$, the strain decreases for the (011) samples, and the (001) samples have the least strain.

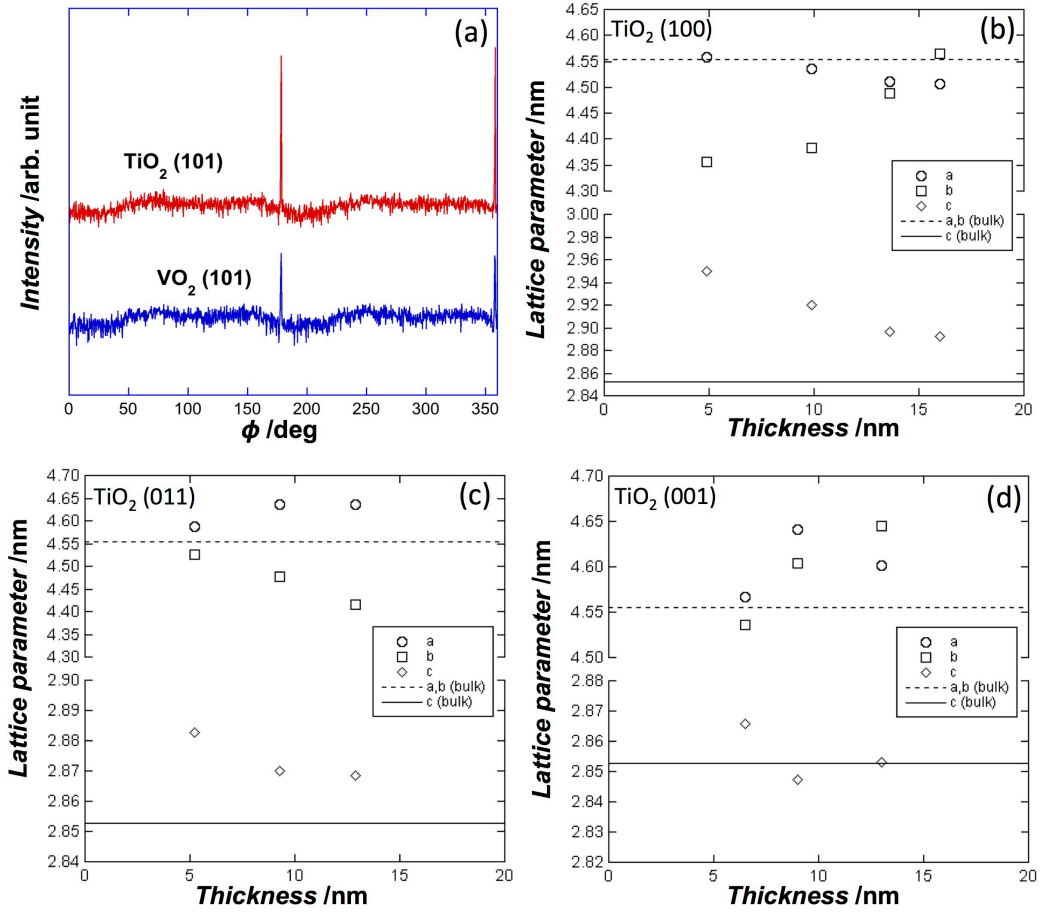


Figure S1. (a) The in-plane ϕ scans of (101) VO₂ and (101) TiO₂. (b)-(d) Lattice parameters as a function of film thickness for VO₂ deposited on (100), (011), and (001) TiO₂ respectively.

Raman spectroscopy revealed that the structure of insulating VO₂ films grown on TiO₂ resembled metallic rutile VO₂, instead of the *MI* structure seen on *c*-plane sapphire. The spectra of VO₂/TiO₂ shown here (before substrate/background subtraction) were dominated by the TiO₂ signal. Even though the *c* lattice parameter (i.e. *c*-strain) varies as a function of film thickness for all of the films grown on *c*-Al₂O₃, the Raman spectroscopy shows only the *MI* phase, and the ω_o peak shifts slightly from 615 to 617 cm⁻¹ as the *c*-strain increases, the peaks are summarized in table II. The tendency of the peak to shift agrees with a previous report on VO₂ microbeams [Atkin, J. M. *et al. Phys. Rev. B* **85**, 020101 (2012).], however the *T* phase and *M2* phase were not observed in our thin films. For the VO₂/TiO₂ samples, only the insulating-*R* phase was observed and does not reveal any shift at room temperature as summarized in **Table S2**.

Table S2. Raman shifts (cm^{-1}) of VO_2 samples

Substrate	Thickness [nm]	Raman shifts [cm^{-1}]				c or b [\AA]*	% "c-strain"
TiO_2 100	4.9	142	232	446	611	2.9493	3.38
	9.9	142	232	446	611	2.9204	2.37
	13.6	142	232	445	611	2.8961	1.52
	16.0	142	233	446	611	2.8924	1.39
TiO_2 011	5.2	142	232	446	611	2.8826	1.05
	9.3	142	233	446	612	2.8699	0.60
	12.9	142	232	446	612	2.8684	0.55
TiO_2 001	6.5	142	231	447	611	2.8660	0.46
	9.0	142	233	445	611	2.8475	-0.19
	13.0	142	233	446	610	2.8529	0.004
Al_2O_3	8.7	195	224	615	750	4.5132	0.17
	12.7	192	224	616	750	4.5028	0.63
	17.0	193	224	617	749	4.5014	0.69

* For samples grown on sapphire, the values are for out-of-plane ‘b’ for *MI* phase. For others, the values are for ‘c’ lattice constant of *R* phase.

The temperature dependence of the *dc* resistivity was measured using a Versa-lab system (Quantum Design), with a heating/cooling rate of 2 K/min, from 280 to 400 K for $\text{VO}_2/c\text{-Al}_2\text{O}_3$, 300 to 400 K for $\text{VO}_2/(100)\text{TiO}_2$, and 250 to 400 K for VO_2 deposited on (001) and (011) TiO_2 substrates. The *dc* resistivity was then calculated according to the device geometry and the thickness of the film, and plotted as a function of temperature as shown in **Figure S2**. The Metal Insulator Transition Temperature (T_{MIT}) of each sample was extracted from the derivative of the logarithm of the resistivity, that is defined as

$$T_{\text{MIT}} = \frac{T_{\text{up}} + T_{\text{down}}}{2}$$

when $T_{\text{up}} = T$ where $\frac{d(\log \rho_{\text{up}})}{dT}$ is at a minimum, and $T_{\text{down}} = T$ where $\frac{d(\log \rho_{\text{down}})}{dT}$ is at a minimum. ρ_{up} is the resistivity from the up-sweep (increasing temperature from 300 to 400 K), and ρ_{down} is the resistivity from the down-sweep (decreasing temperature from 400 to 300 K).

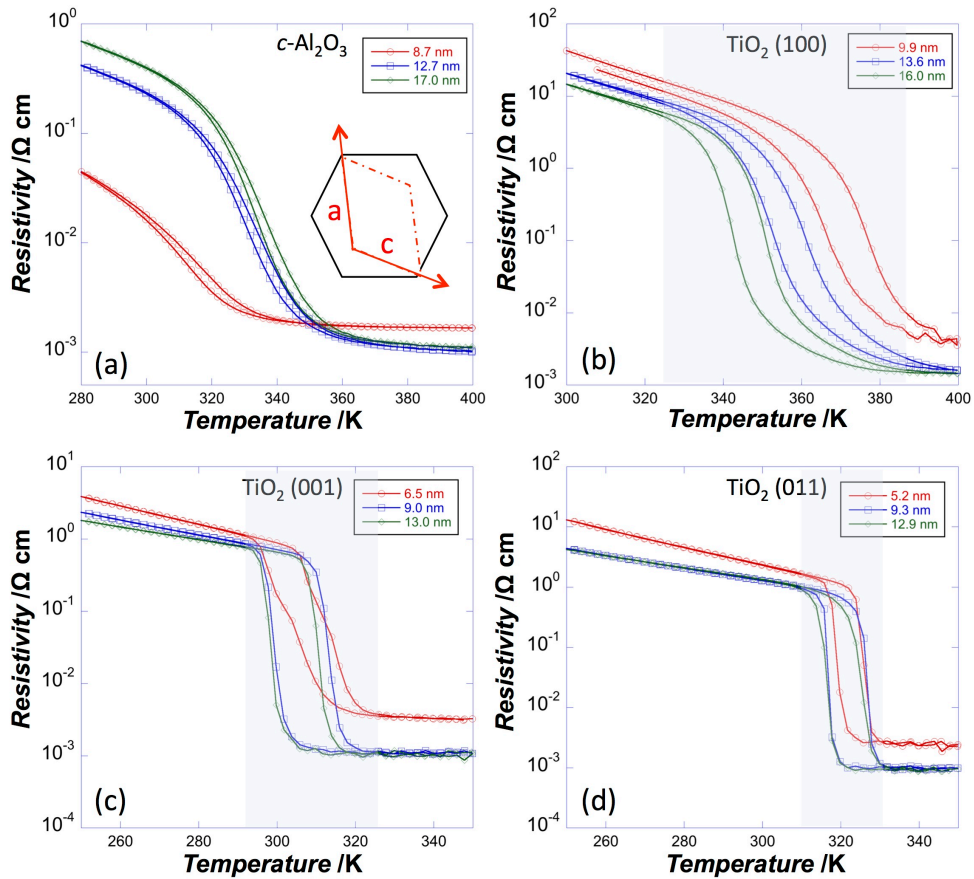


Figure S2. (a)-(d) Resistivity as a function of temperature of various thickness VO₂ deposited on *c*-Al₂O₃, (100), (001), and (011) TiO₂ respectively, inset showing monoclinic structure of VO₂ (red dash line) on top of hexagonal crystal structure of *c*-Al₂O₃ (black solid line), the highlighted area showing a possible two phase region.

All the TiO₂ samples preserve the resistivity ratio during the transition very well, ~3-4 orders of magnitude, while the *c*-Al₂O₃ samples experience great suppression as the film get thinner as shown in figure S2. This due to the fact that the films grown on *c*-Al₂O₃ substrates are not epitaxial, since the crystal structure of the substrate is hexagonal, and the crystal structure of VO₂ is monoclinic (as shown in figure S2a inset). The different crystal structures, together with the large lattice mismatch, results in poorer VO₂ crystallinity as compared to the epitaxial VO₂ grown on TiO₂ substrates.

Being the most strained films, the VO₂/(100) TiO₂ samples experience the largest shift in the transition temperature (T_{MIT}) as the thickness varies, on the other hand, the thickness has a minimal effect on the *c*-strain and the T_{MIT} for (011) and (001) samples. For the (100) samples the *c*-mismatch is much larger than the *a*-mismatch, hence these samples get the largest (in-plane) strain from the substrate clamping effect, and thus relax much faster than the (011) samples and the (001) samples. Being less strained, thus better crystallinity, the (011) samples

and the (001) samples show much sharper transitions than the (100) or the c -Al₂O₃ samples. There is also a signature of more defects in the thinner films, as the resistivity in the metallic phase is higher than the thicker films as seen in figure S2. Interestingly, the 6.5 nm (001) film also shows a two-step transition, suggesting multiple phases with different transition temperatures, while this is not the case for the (011) film deposited at the same condition.

The phase diagram presented in the manuscript was constructed according to previous reports on transport anisotropy and the highlighted area of coexistence as shown in Figure S2; i.e. the coexistence temperature range of the (100) TiO₂ samples is about ± 30 K, note that the resistivity measurement was done along the c -axis in which the T_{MIT} is 3-5 K higher than the T_{MIT} along the in-plane a -axis, resulting in a 30 K lower bound and 35 K upper bound for the two phase region.